# XRD AND HREM STUDIES OF NANOCRYSTALLINE Cu AND Pd

G. W. NIEMAN*, J. R. WEERTMAN*, AND R. W. SIEGEL**
* Department of Materials Science and Engineering, Northwestern University, Evanston, IL 60208
** Materials Science Division, Argonne National Laboratory, Argonne, IL, 60439

## ABSTRACT

Consolidated powders of nanocrystalline Cu and Pd have been studied by x-ray diffraction (XRD) and high resolution electron microscopy (HREM) as part of an investigation of the mechanical behavior of nanocrystalline pure metals. XRD line broadening measurements were made to estimate grain size, qualitative grain size distribution and average long range strains in a number of samples. Mean grain sizes range from 4-60 nm and have qualitatively narrow grain size distributions. Long range lattice strains are of the order of 0.2-3% in consolidated samples. These strains apparently persist and even increase in Cu samples after annealing at 0.35 Tm (498K) for 2h, accompanied by an apparent increase in grain size of ≥2x. Grain size, grain size distribution width and internal strains vary somewhat among samples produced under apparently identical processing conditions. HREM studies show that twins, stacking faults and low-index facets are abundant in as-consolidated nanocrystalline Cu samples. Methodology, results and analysis of XRD and HREM experiments are presented.

## INTRODUCTION

X-ray diffraction (XRD) line broadening studies and high resolution electron microscopy (HREM) have been performed as part of our ongoing study of the mechanical properties of nanocrystalline metals. A more detailed description of our XRD studies is given in reference (1). Line broadening has been used primarily to obtain an accurate estimate of the mean grain size of the powders produced by inert gas condensation and consolidated for use in mechanical properties tests (reviewed in these proceedings (2).) Estimates of the mean long range distortion with respect to the average lattice were also obtained from this analysis. The basis for estimating average grain size and lattice strain of a powder or polycrystalline sample by XRD line broadening methods has been well-discussed (3-5). Analysis is possible for samples having a grain size smaller than about 100 nm and containing small to moderate long range strains. Recent studies of nanocrystalline samples produced by several methods have have measured average sizes in the range of 5-25 nm by XRD and TEM methods (6,7). Results of such studies must be considered carefully, since different estimation methods may give different grain size/strain estimates based on the weighting factors of the method, its inherent assumptions, and other factors. We have used HREM studies of consolidated and unconsolidated nanocrystalline Cu samples to obtain information about twinning, dislocations, grain size distributions, and strains. These direct observations of nanostructure complement the XRD studies to give an understanding of the complexity involved in determining the grain size-dependence of mechanical properties in ultrafine-grain materials.

Mat. Res. Soc. Symp. Proc. Vol. 206. ©1991 Materials Research Society

https://doi.org/10.1557/PROC-206-493 Published online by Cambridge University Press

## XRD ESTIMATES OF GRAIN SIZE AND STRAINS

Domain size, lattice distortion, and instrumental effects all cause broadening of XRD lines. Instrumental effects can be removed by subtraction of the diffraction profile for a well-annealed coarse-grain standard from the experimental profile (3,4). Analysis of the remaining broadening then provides an estimate of the mean grain size, d, which is independent of the scattering angle $\theta_B$, and, using two or more orders of a particular reflection (ex. 111 and 222), of mean long range strain, $<\varepsilon^2>^{1/2}$, which is proportional to $\tan\theta_B$. The grain size estimate is based on the determination of the coherent scattering length normal to the diffracting plane. Twin boundaries and stacking faults may look like true grain boundaries if they interrupt the coherent scattering. Two grain size/strain estimation methods are commonly employed. The Warren-Averbach (WA) Fourier method (3-5) provides an area-weighted grain size estimate. The Fourier coefficients are calculated from the full diffraction line profile, which must be measured over several line widths on either side of the peak maximum. The Scherrer method (3,5) provides a volume-weighted average based on the full-width-half-maximum (fwhm) of the diffraction profile. The fwhm is obtainable by numerical methods, fitting the experimental diffraction profile by a pseudo-Voigt or Pearson VII function (e.g., 9). This profile modelling technique is also useful for extending the tails of higher order peaks when overlap between two peaks occur (e.g., 311 and 222 in fcc metals). Comparison of volume- and area-weighted averages gives a qualitative estimate of the width of the grain size distribution, since the volume-weighted average weights larger grain sizes more heavily than the area-weighted average. In principle this distribution is obtainable from the second derivative of the Fourier coefficients with respect to scattering domain length, but data quality usually precludes this for conventional XRD profiles (3,10).

The samples used in this study were 9 mm diameter disks consolidated from powders of nanocrystalline Cu and Pd produced by inert gas condensation (11,12). All samples were evaporated at or near the melting temperature of the metal into ≈ 760 Pa of He gas. A 9 mm diameter well-annealed sample with a grain size of ≈ 50 μm was used to obtain the instrumental broadening function for each XRD session. XRD profiles from 111-222 diffraction lines were collected digitally using a custom-built diffractometer with monochromated $K_{\alpha 1}$ radiation. The Fourier coefficients for the experimental profiles were corrected for instrumental broadening using the Stokes correction (3,4). Subsequently, the data for each diffraction profile were normalized using the method of Rothman and Cohen (13), and the grain size and mean long-range strains were calculated in the usual way (1,3,4,13).

Average grain size and strain data for 11 as-consolidated samples of nanocrystalline Pd and Cu are shown in Table 1 to illustrate the grain size, grain size distribution and strain data obtained from the XRD analyses described above. The grain size and long range strain were redetermined for 3 Cu samples after annealing in vacuum for 2h at 100°C and subsequently at 200°C for 2h. These results are shown in Table 2. Area-averaged grain size estimates for Pd samples range from 3-21 nm with mean long range strain estimates ranging from 1-34 x $10^{-3}$. For Cu samples, grain size ranges from 4-60 nm with strains of 0-12 x $10^{-3}$. Size estimates for the 111 and 200 profiles generally agree well with each other and with the double peak estimate for the sample, but in general, single peak estimates are a little smaller than double peak estimates. The Scherrer method

https://doi.org/10.1557/PROC-206-493 Published online by Cambridge University Press

grain size estimates are a factor of ≈ 2-5 larger than the Fourier estimates, indicating that the grain size distribution varies in width from sample to sample. The strain estimates obtained are of the same order of magnitude as for cold-worked metals (13,14) and ceramic materials (7) in the 5-100 nm grain size range. The data show no apparent relationship between grain size and the magnitude of the mean strain (1).

The data for the annealed samples in Table 2 show that the original samples had a significantly wide grain size distribution, since the Scherrer and WA double peak data differ by a factor of 3. After the 100°C anneal, the mean grain size apparently increased by less than about a factor of 2, while long range strains increased significantly. After the anneal at 200°C the grain size increased by a factor of 2-7 over the original grain size, while strains apparently remained larger than in the as-compacted sample. The grain size results are consistent with the expectation of grain growth at elevated temperature, and $(D_v t)^{1/2} < \Delta d < (D_v t)^{1/3}$, for the grain size increase, $\Delta d$, and bulk diffusivity $D_v$ (calculated at 200°C, as in ref.(15).) The long range strain data are more difficult to explain. This strain should be relieved in ≈1h at about 150°C in pure Cu. Perhaps these strains are localized at the sample surface and are atypical of the bulk. Alternatively, a better understanding of the resolution limits of the strain calculation may explain these observations; or of the effects of annealing the complex nanostructure (with abundant multiple twins and stacking faults) on the partitioning of broadening into the grain size ($A_{ns}$) and strain ($A_{nd}$) components of the Fourier coefficients, $A_n = A_{ns}(hkl)A_{nd}(hkl)$.

***Table I.*** *Comparison of mean grain size (nm) estimates for as-consolidated samples, obtained by several methods, and mean long range strains ($\langle \varepsilon_{10}^2 \rangle^{1/2}$) calculated at 10 Å scattering length from WA double peak XRD data. (After ref. 1)*

| Sample | Scherrer* | Single-peak 111 peak | Single-peak 200 peak | Double-peak | $\langle \varepsilon_{10}^2 \rangle^{1/2}$ ($\times 10^{-3}$) |
|---|---|---|---|---|---|
| Pd7061[a] | 54 | 11 | | 11 | 1.4 |
| Pd8051[a] | 7 | 3 | | 3 | 2.2 |
| Pd8101[b] | 30 | 5 | 6 | 21 | 34.0 |
| Pd12031[a] | 28 | 12 | | 8 | 3.2 |
| Pd12051[a] | 8 | 5 | | 5 | 3.9 |
| Cu2232[a,c] | 15 | 5 | 5 | 5 | 3.1 |
| Cu2261[a] | 20 | 6 | 4 | 6 | 0.6 |
| Cu3012[a] | 30 | 10 | 7 | 15 | 12.0 |
| Cu3021[a,c] | 28 | 7 | 6 | 7 | 3.4 |
| Cu3051[a,d] | 69 | 59 | | 59 | 0.0 |
| Cu3071[a,d] | 88 | 10 | 10 | 10 | 2.7 |

[a] = 111-222 peaks used for double-peak analysis
[b] = 200-400 peaks used for double-peak analysis
[c] = samples consolidated in air
[d] = samples evaporated from a $Cu_7$-Si alloy
* = determined from 111 line full-width-half-maximum

https://doi.org/10.1557/PROC-206-493 Published online by Cambridge University Press

***Table 2.*** *Comparison of grain size (nm) and mean long range strains ($<\varepsilon_{10}^2>^{1/2}$) estimates for as-consolidated Cu samples, and for the same samples following annealing at 100 and 200 °C. See Table 1 for further explanation.*

| Sample | Scherrer* | Single-peak 111 peak | Single-peak 200 peak | Double-peak | $<\varepsilon_{10}^2>^{1/2}$ (x $10^{-3}$) |
|---|---|---|---|---|---|
| Cu2221[a] | 21 | 6 | 4 | 6 | 1.8 |
| Cu2221[b] | 42 | 12 | 7 | 14 | 3.4 |
| Cu2221[c] | 53 | 27 | 24 | 38 | 4.0 |
| Cu2271[a] | 17 | 6 | 4 | 6 | 1.0 |
| Cu2271[b] | 21 | 8 | 7 | 9 | 8.1 |
| Cu2271[c] | 53 | 22 | 16 | 14 | 2.8 |
| Cu3091[a] | 30 | 8 | 6 | 8 | 1.5 |
| Cu3091[b] | 24 | 10 | 6 | 11 | 4.9 |
| Cu3091[c] | 32 | 18 | 14 | 24 | 4.5 |

a = as-consolidated samples
b = samples annealed in vacuum for two hours at 100°C
c = samples annealed in vacuum for two hours at 200°C
* = determined from 111 line full-width-half-maximum

## HREM OBSERVATIONS OF NANOCRYSTALLINE CU SAMPLES

We have made HREM observations of several samples of nanocrystalline Cu to gain some insight into nanostructural features that influence mechanical properties and affect grain size and strain estimates made by XRD methods. All observations were made on the Hitachi H9000 microscope at Northwestern University, which operates at 300 kV. The consolidated samples were prepared by mechanical polishing, followed by jet polishing in a solution of 70% H2O and 30% $H_3PO_4$ at approximately 5°C, using 10 V and ≥ 100 mA. The samples were viewed such that the electron beam direction was approximately parallel to the axis of compression during sample consolidation. The many difficulties in making high-quality HREM observations, and the necessity of complementary image simulations to knowing well the relation between an image and the true material structure, are well-discussed (16,17). Examples of nanostructural features frequently observed in our samples, such as multiple twinning and low-index faceted crystals, can be presented without such evidence, however, to show characteristics of the complex nanostructure.

Typical high resolution images of sample Cu2221 in the as-consolidated state are shown in Figs. 1 and 2a, illustrating the abundance of twinning and of low-index, faceted crystal regions. Dislocations are rarely seen, but this may be due to the stringent conditions needed for their observation in HREM (16). A detailed image of the crystal in the lower left of Fig. 1 is shown in Fig. 2a with the multiple twin planes indicated by the arrows. Fig. 2b shows an example of a twinned, faceted crystal region in as-consolidated sample Cu3012. In addition to twins and stacking faults in Fig. 1, there is considerable overlap among crystals that obscures the definition crystal boundaries. Determination of grain sizes by TEM would seem to demand some subjectivity, since even dark-field diffraction conditions will be influenced by overlap and crystal defects. The influence of the

https://doi.org/10.1557/PROC-206-493 Published online by Cambridge University Press

twins and stacking faults observed by HREM on XRD-estimated grain sizes is not clear, although the crystal/domain sizes observed here are in general somewhat larger than the size estimates made by the WA method. Nevertheless, grain sizes observed by HREM are in the range of the grain size estimates made by XRD for different diffraction conditions and by different XRD methods, shown in Table 1. Simplifying assumptions about nanostructure (e.g. coherent scattering length normal to (111) = grain size) and about analytical methodology (e.g. long range strains are small), as well as statistical errors, are inherent in the separation of line broadening components to estimate grain size and strain by XRD methods. These complexities suggest that relationships between estimated nanocrystalline grain size and macroscopic to microscopic physical properties measurements should be identified cautiously.

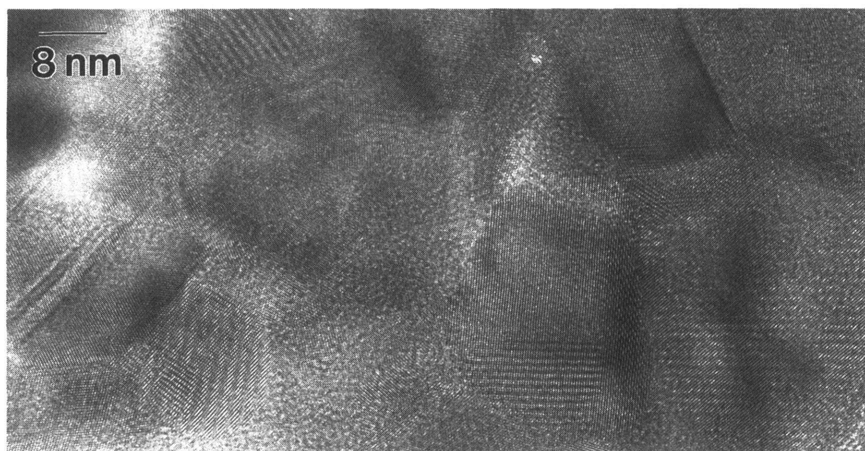


*Fig. 1. Example of microstructure in nanocrystalline Cu sample Cu2221.*

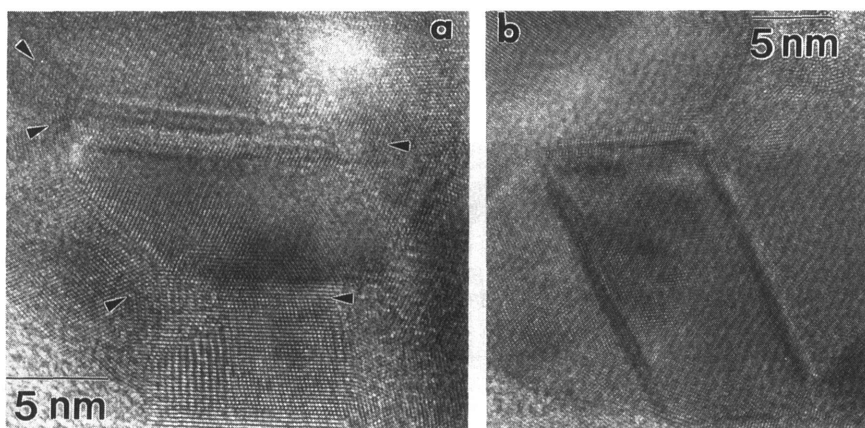


*Fig. 2. Details of twinned crystals with low index plane facets in samples (a) Cu2221 and (b) Cu3021.*

https://doi.org/10.1557/PROC-206-493 Published online by Cambridge University Press

We are in the process of making more complete HREM observations that may help us to better understand the importance of grain size, twinning, stacking faults and dislocations in the nanostructure of ultrafine-grain metals as this nanostructure evolves through stages of synthesis, consolidation, and controlled deformation. This understanding should lead quickly to development of useful applications of nanocrystalline materials.

## ACKNOWLEDGEMENTS

Research at Northwestern University was supported by the NSF, grant number DMR-8320157, and made use of facilities supported by the Materials Research Laboratory program of NSF, grant number DMR-8821571. The work at Argonne National Laboratory (ANL) was supported by the U. S. Department of Energy, BES-Materials Sciences, under Contract W-31-109-Eng-38. We thank Dr. J. A. Eastman and Y. X. Liao at ANL and Drs. J. Barker and P. Georgopoulos at NU for discussions.

## REFERENCES CITED

1 G. W. Nieman and J. R. Weertman, Proc. M. E. Fine Symp., ASM/TMS Annual Mtg., Detroit (1990), in press.
2 Nieman, G. W., Weertman, J. R., and Siegel, R. W., this symposium (1990).
3 B. E. Warren, *X-ray Diffraction*, (Addison-Wesley, Reading, MA,1969) pp. 251-275.
4 L. H. Schwartz and J. B. Cohen, *Diffraction from Materials*, 2nd ed.,(Springer-Verlag, Berlin,1987) pp. 372-402.
5 A. Guinier, *X-ray Diffraction In Crystals, Imperfect Crystals and Amorphous Bodies*, (W. H. Freeman and Co., San Francisco, 1970) pp. 121-142.
6 E. Hellstern, H. J. Fecht, Z. Fu, and W. L. Johnson, J. Appl. Phys. 65, 305 (1989).
7 J. S. C. Jang and C. C. Koch, Scripta Met. et Mater. 24, 1599 (1990).
9 R. A. Young and D. B. Wiles , Adv. X-ray Anal. 24, 1 (1981); J. Appl. Cryst. 15, 430 (1982).
10 S. Enzo, G. Fagherazzi, A. Benedetti and S. Polizzi, J. Appl. Cryst. 21, 536 (1988).
11 G. W. Nieman, J. R. Weertman, and R. W. Siegel, submitted for publication (1990).
12 C. G. Granqvist and R. A. Buhrman, J. Appl. Phys., 47, 2200-2219 (1976).
13 R. L. Rothman and J. B. Cohen, in *Advances in X-Ray Analysis,* J. B. Cohen and others, eds., 12, 208 (1969).
14 R. K. Nandi, H. K. Kuo,W. Schlosberg, G. Wissler, J. B. Cohen and B. Crist, J. Appl. Cryst. 17, 22 (1984).
15 H. J. Frost and M. F. Ashby, *Deformation Mechanism Maps: The Plasticity and Creep of Metals and Ceramics*, (Springer-Verlag, Berlin,1989) pp. 20-27.
16 G. J Wood, W. M. Stobbs and D. J. Smith, Phil. Mag. 50A, 375 (1984).
17 P. Pirouz and F. Ernst, in *Metal-Ceramic Interfaces*, M. Rühle et al., eds. (Pergamon Press, Oxford,1989) pp. 199-221.

https://doi.org/10.1557/PROC-206-493 Published online by Cambridge University Press